

L. D. Keigwin · J. P. Sachs · Y. Rosenthal

## A 1600-year history of the Labrador Current off Nova Scotia

Received: 11 June 2002 / Accepted: 3 January 2003 / Published online: 8 April 2003  
© Springer-Verlag 2003

**Abstract** A multicore from Emerald Basin, on the continental margin off Nova Scotia, has a modern  $^{14}\text{C}$  age at the top, and other  $^{14}\text{C}$  dates indicate a linear sedimentation rate of  $\sim 30$  cm/ka to 1600 calendar years BP. This rate is great enough to record century-to-millennial scale changes in the surface and deep ( $\sim 250$  m) waters in the basin that are influenced by the Labrador Current. We applied five proxies for seawater temperature changes to the sediments of Emerald Basin, including the percent abundance and the oxygen isotope ratio ( $\delta^{18}\text{O}$ ) of the polar planktonic foraminifer *N. pachyderma* (s.), the unsaturation ratio of alkenones ( $U^{k_{37}}$ ) produced by prymnesiophyte phytoplankton, and the  $\delta^{18}\text{O}$  and Mg/Ca of benthic foraminifera. All five proxies indicate the ocean warmed suddenly sometime in the past 150 years or so. The exact timing of this event is uncertain because  $^{14}\text{C}$  dating is inaccurate in recent centuries, but this abrupt warming probably correlates with widespread evidence for warming in the Arctic in the nineteenth century. Because the Canadian Archipelago is one of the two main sources for the Labrador Current, warming and melting of ice caps in that region may have affected Labrador Current properties. Before this recent warming, sea surface temperature was continually lower by 1–2 °C, and bottom water was colder by about 6 °C in Emerald Basin. These results suggest that there was no Medieval Warm

Period in the coastal waters off Nova Scotia. Because there is also no evidence of medieval warming in the Canadian archipelago, it seems likely that coastal waters from Baffin Bay to at least as far south as Nova Scotia were continually cold for  $\sim 1500$  of the past 1600 years.

### 1 Introduction

Emerald Basin is a 250 m deep depression on the continental shelf about 60 nautical miles south of Halifax, N.S. (Fig. 1). Like many basins along formerly glaciated margins, it is filled with a thick sequence of post-glacial sediments (King and Fader 1986). Because Emerald Basin is so close to Halifax and the Bedford Institute of Oceanography, its sediments have been cored dozens of times. In general, such sampling has been to test various coring tools, and to determine the physical properties of the sediments that give such distinctive acoustic reflections (King and Fader 1986). This basin is of further interest because its hydrography has been sampled often since the late 1940s, and it has a nearly continuous monthly series of surface to bottom water properties since about 1950. These results illustrate the extremely high interannual variability in sea surface temperature (SST) of this part of the western North Atlantic as well as the high interdecadal variability that is probably related to transport variability of the Labrador Current (Petrie and Drinkwater 1993).

Despite the high rates of sedimentation, and the strong ocean and climate signal, a high resolution record of paleoclimate for Emerald Basin is not available. Previous work by paleoceanographers noted abundant and diverse benthic and planktonic foraminifera (Vilks and Rashid 1976; Scott et al. 1984), yet these authors sampled their cores at 100 cm and 50 cm spacing, respectively. Recently, a high resolution Holocene record of pollen and dinocyst data have become available from nearby La Have Basin (Levac 2001). While not exactly comparable to the geochemical results presented here,

---

L. D. Keigwin (✉)  
Department of Geology and Geophysics,  
Woods Hole Oceanographic Institution,  
Woods Hole, MA 02543, USA  
E-mail: Lkeigwin@whoi.edu

J. P. Sachs  
Department of Earth, Atmospheric and Planetary Sciences,  
Massachusetts Institute of Technology,  
77 Massachusetts Avenue, Room E34-254,  
Cambridge, MA 02139, USA

Y. Rosenthal  
Institute of Marine and Coastal Sciences,  
and Department of Geology, Rutgers, The State University,  
71 Dudley Road, New Brunswick, NJ 08901-8521, USA

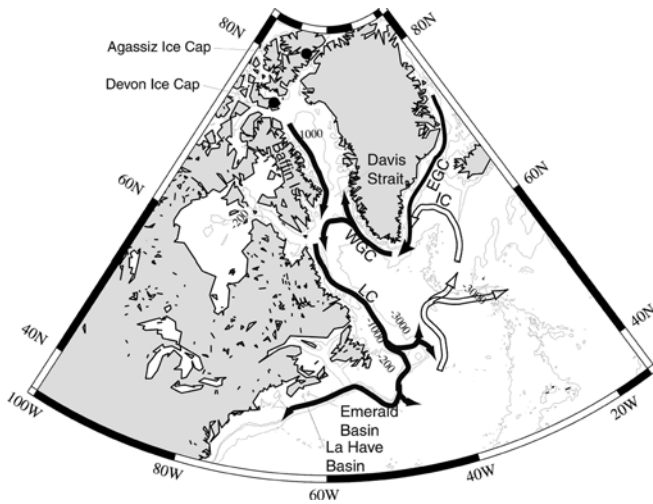


**Fig. 1** Location of Emerald Basin on the Scotian Shelf, with respect to nearby La Have Basin and surface ocean currents. Currents of northern and southern origin are shown in *black*, and *white*, respectively, and isobaths are indicated at 200, 1000, and 3000 m. *EGC* is East Greenland Current, *WGC* is West Greenland Current, *IC* is Irminger Current, *LC* is Labrador Current

those data indicate near-constant summer SSTs of 16–17 °C during most of the last ~1500 years, with a sudden warming of 2.5 °C within the last few centuries, followed by an equally large and abrupt cooling at the core top (see Levac 2001, Fig. 7). We sampled Emerald Basin with a multicorer (MC) on cruise 326 of R/V *Oceanus* in July 1998. MC-29 came from 45°53.1003'N, 62°47.7009'W at 250 m. We have developed paleotemperature and paleosalinity estimates for Emerald Basin surface and deep waters using five geochemical and micropaleontological methods. Results show large and abrupt warming of Emerald Basin surface and deep waters coincident with the end of the Little Ice Age in the middle of the nineteenth century. This sudden change correlates with widespread evidence for warming in the Arctic region (Overpeck et al. 1997), the source of the Labrador Current, and followed at least 1500 years of continuously cold and fresh conditions.

## 2 Methods

### 2.1 Sediment core sampling

MC-29D was extruded from the core liner, sliced into one cm intervals along its 50 cm length, and refrigerated in plastic bags. Samples of about 5 to 10 g (dry) were removed from the bags and washed over a 63 µm screen. Splits were put aside for counting the planktonic foraminifera *N. pachyderma* (sinistral) and lithic grains (> 150 µm), and the remainder of the coarse fraction was used for geochemical studies of foraminifera.

### 2.2 Alkenone paleothermometry

Samples of ~2 g (dry) were removed from the bags for alkenone analyses, which followed the procedures of Sachs and Lehman (1999). In brief, samples were stored frozen at –20 °C and

freeze-dried prior to extraction. After drying, ~2 g sediment was weighed, and an equivalent quantity of sodium sulfate plus a recovery standard, ethyl triacetoate, were added. The mixture was loaded into a stainless steel cell and extracted on a Dionex ASE-200 pressurized fluid extractor with methylene chloride. The solvent was evaporated on a Zymark Turbovap II and the lipid extract transferred to a 2 ml autosampler vial. The extract was redissolved in toluene containing the quantitation standard, *n*-hexatriacontane, and derivatized with bis(trimethylsilyl)trifluoroacetamide at 60 °C for 1 h.  $C_{37}$  methyl ketones (alkenones) were quantified by capillary gas chromatography on a Hewlett Packard 6890 using a Chrompack CP-Sil-5 60 m × 0.32 mm i.d. column, a programmable temperature vaporization inlet, and flame ionization detector, all controlled by Hewlett Packard Chemstation software. A Bermuda Rise sediment standard, prepared from a mixture of late Pleistocene glacial and interglacial material, was extracted after every 30 authentic samples. Its  $U^{k}_{37}$  was determined twice, with 15 samples run between analyses. The standard deviation of many repeated analyses indicate a precision of 0.007  $U^{k}_{37}$  units, or 0.2 °C using the Prahl et al. (1988) temperature calibration.

Numerous studies have demonstrated that sedimentary  $U^{k}_{37}$  is a useful proxy for mean annual SST at 0 m water depth in the temperature range 0°–29 °C (Müller et al. 1998, and references therein). Global core top calibrations of the alkenone paleothermometer (Müller et al. 1998) are nearly identical to the original temperature calibration, which we use here, based on cultures of *E. huxleyi* (Prahl et al. 1988). The appropriateness of this calibration for Emerald Basin is supported by the core-top (0–1 cm) alkenone SST of 8.8 °C, which is nearly identical to the 48-years average measured SST (1947–1995) in Emerald Basin at 0 m, 8.7 °C (data from Ken Drinkwater, Bedford Institute of Oceanography, personal communication to LDK).

### 2.3 $^{210}\text{Pb}$ analyses

Samples were also taken for  $^{210}\text{Pb}$  dating in the laboratory of K. Buesseler at Woods Hole. These were disaggregated in a beaker with distilled water on a shaker table, settled and dried. Broken pieces of the dried residue were removed to leave exactly 2 g. Samples were again disaggregated as described already and settled, but not allowed to dry completely. We used this method to avoid grinding the samples, yet to achieve samples of identical mass, with an unbiased size distribution of particles, and with a uniform distribution on the flat bottom of the beaker used for gamma counting.

### 2.4 Stable isotope analyses

About 15 individuals of *N. pachyderma* (s.) (150–250 µm) and individuals of the benthic foraminifer *Cibicides lobatulus* were picked for stable isotope analysis. Analyses were conducted on a partially automated VG 903 mass spectrometer with a high sensitivity source. Results are calibrated to PDB using the standard NBS-19.

### 2.5 Mg/Ca analyses

About ten individuals of *C. lobatulus* were used for Mg/Ca analysis. Additionally, *C. pachyderma* were analyzed in the top 3 cm. The samples were cleaned using a protocol to remove clays, organic matter and metal oxides (Boyle and Keigwin 1985/86). Then, foraminiferal shells were gradually dissolved in trace metal clean 0.065 N  $\text{HNO}_3$  (OPTIMA) and 100 µl of this solution was diluted with 300 µl trace metal clean 0.5 N  $\text{HNO}_3$  to obtain a Ca concentration of  $3 \pm 1 \text{ mmol l}^{-1}$ . Measurements of Mg/Ca were done at Rutgers University by Finnigan MAT Element Sector Field Inductively Coupled Plasma Mass Spectrometer (ICP-MS)

operated in low resolution ( $m/\Delta m = 300$ ) following the method outlined in Rosenthal et al. (1999). Instrument precision was determined by repeated analysis of three consistency standards. The precision of the consistency standard with Mg/Ca of 1.10 and  $2.40 \text{ mmol mol}^{-1}$  were  $\pm 3.7\%$  and  $\pm 1.5\%$  (r.s.d.), respectively. Bottom water temperatures (BWTs) were calculated using the newly revised equation for *Cibicidoides* species:  $\text{Mg/Ca} = 0.867 \pm 0.049 \exp(0.109 \pm 0.007 \times \text{BWT})$  (Lear et al. in press).

## 2.6 $^{14}\text{C}$ analyses

Accelerator mass spectrometer (AMS)  $^{14}\text{C}$  measurements were made at the National Ocean Sciences AMS (NOSAMS) facility at Woods Hole. Because of low planktonic foraminiferal abundance near the core top, the analysis there was on mixed species of benthic foraminifera. At deeper levels in the core we were able to date mixed planktonic foraminifera.

## 3 Results

### 3.1 Chronology

Samples for AMS dating (Table 1) were largely chosen based on the % *N. pachyderma* curve (see later). The  $^{14}\text{C}$  result on mixed benthic foraminifera at the core top, 375 conventional  $^{14}\text{C}$  years, is essentially a zero age because waters at 200 m depth in this part of the western North Atlantic are at least that old (Chris Weidemann, personal communication to LDK 2000). Two additional dates on mixed planktonic foraminifera at 12.5 and 14.5 cm are also effectively zero age because the conventional  $^{14}\text{C}$  ages are less than the surface reservoir age of 400 years. By 16.5 cm down the core, we found the first “non-zero” age that could be calibrated to years BP, and below that the age increased regularly to  $\sim 1600$  years at 49.5 cm. An age model using a linear fit to zero age at the core top and the underlying calendar ages (Table 1) results in a sedimentation rate of 30 cm/ka. This age model (Fig. 2) is consistent with results obtained deeper in Emerald Basin in other studies (Piper and Fehr 1989).

To constrain better the age model near the core top, we also measured  $^{210}\text{Pb}$  in MC-29. Excess  $^{210}\text{Pb}$  is present as deep as 20 cm in these samples, with some suggestion of higher activities between 5.5–11.5 cm (Fig. 2).  $^{137}\text{Cs}$  was not detected in our samples. Although these higher activities may indicate episodes of accelerated sedimentation existed during part of the

last one or two centuries at this location, this depth distribution of  $^{210}\text{Pb}$  is typical of many locations worldwide (W. Martin, WHOI, personal communication to LDK 2002).

### 3.2 Sedimentology

In the process of counting foraminifera for SST estimation, we derived the total number of planktonic foraminifera/g as well as terrigenous grains  $>150 \mu\text{m}$ . Throughout most of MC-29 the abundance of planktonic foraminifera is variable but high, but it drops suddenly in the upper 2 cm to numbers close to 10/g (Fig. 3a). Terrigenous grains, which may have been ice rafted to this location, are much less common than planktonic foraminifera (Fig. 3a). The abundance of

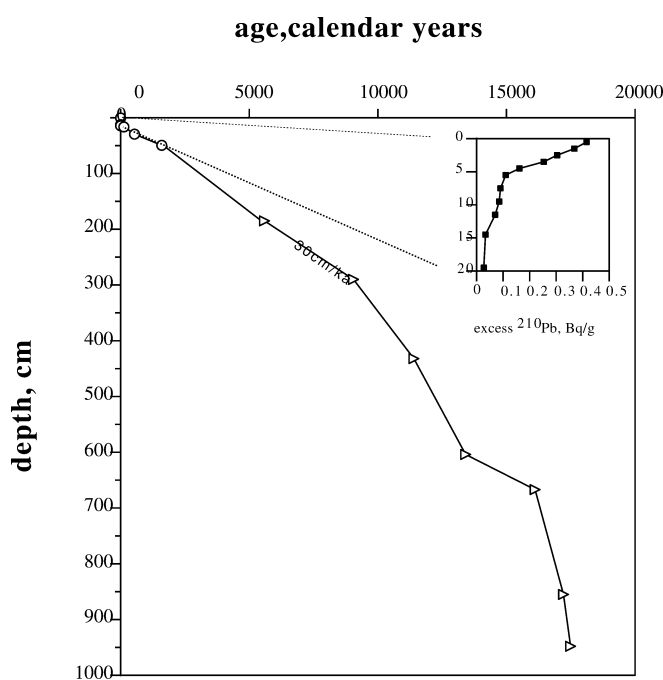


**Fig. 2** Age-depth relationship of Emerald Basin sediments. Circles are results of AMS accelerator dates on foraminifera from Oceanus 326 MC29D (Table 1), and triangles are macrofossil dates of Piper and Fehr (1991) from a nearby piston core. For most of the Holocene, the sedimentation rate was close to 30 cm/kyr, although our AMS dates and our excess  $^{210}\text{Pb}$  results (inset) are consistent with a higher rate near the core top

**Table 1** Radiocarbon results on foraminifera from OCE326 MC-29D, Emerald Basin

Depth interval	Depth	Species	Accession #	Conventional $^{14}\text{C}$ age	Error, $1\sigma$	Reservoir Corrected age	Calendar age, years	$1\sigma$ age range
0–1	0.5	mixed BF	OS-20560	375	30	0	0	
12–13	12.5	mixed PF	OS-27370	255	60	0	0	
14–15	14.5	mixed PF	OS-27369	375	60	0	0	
16–17	16.5	mixed PF	OS-27393	505	120	105	127	275 to 0
29–30	29.5	mixed PF	OS-27372	960	70	560	540	619 to 504
49–50	49.5	mixed PF	OS-25803	2040	60	1640	1599	1686 to 1527

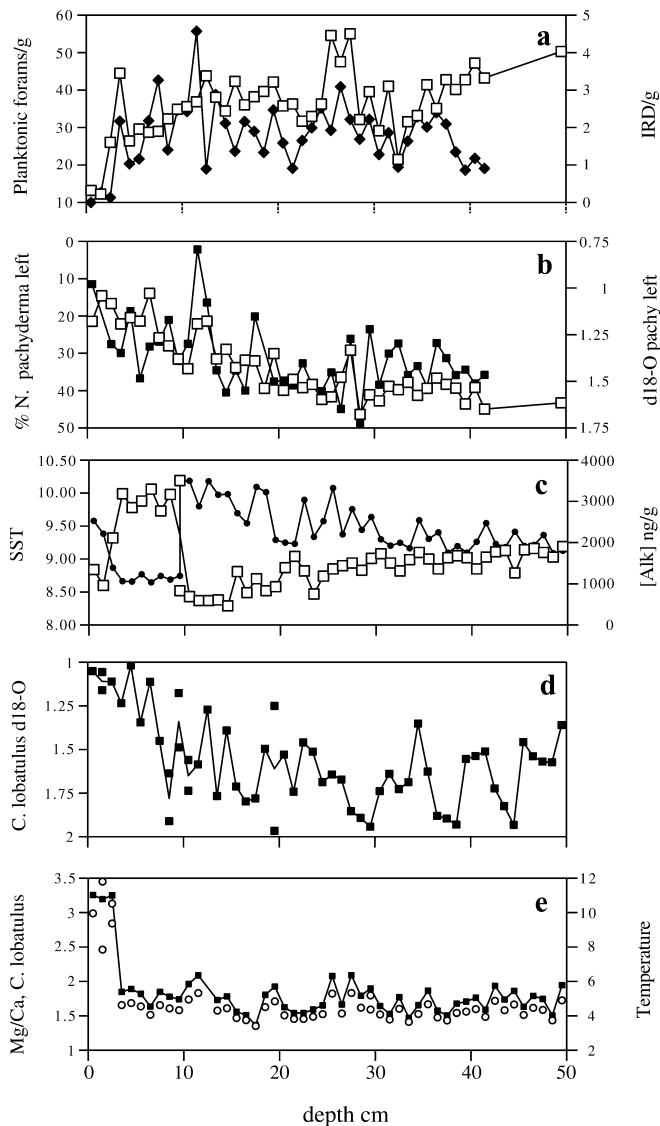


**Fig. 3a–e** Sedimentological, micropaleontological and geochemical results at core OCE326 MC29D. **a** Abundance of planktonic foraminifera (*squares*) and lithic grains (*diamonds*)  $>150\ \mu\text{m}$ ; **b** percent abundance of the polar planktonic foraminifer *N. pachyderma* (s.) (*open squares*) and its  $\delta^{18}\text{O}$  (*solid squares*); **c** concentration of alkenones in dry sediment (*solid circles*), and SST based on alkenone unsaturation (*open squares*); **d**  $\delta^{18}\text{O}$  of the benthic foraminifer *C. lobatulus*; **e** Mg/Ca in *C. lobatulus* (*open*), and the bottom water temperature based on Mg/Ca (*solid*)

these grains falls below background levels in the top few cm of the core, and they are completely absent from the core top.

### 3.3 *N. pachyderma* abundance

The polar planktonic foraminifer *N. pachyderma* averages about 40% of the planktonic fauna in the lower 20 cm of MC-29 (Fig. 3b). Exactly where above 30 cm the *N. pachyderma* decreases significantly is difficult to say, but by 20 cm the abundance is down to  $\sim 30\%$ , and by 10 cm it is  $<20\%$ .

### 3.4 Stable isotopes

Both planktonic (Fig. 3b) and benthic foraminifera (Fig. 3d) show a 1 permil range in  $\delta^{18}\text{O}$ , and for each  $\delta^{18}\text{O}$  decreases near the core top. Below  $\sim 17\ \text{cm}$ ,  $\delta^{18}\text{O}$  of *N. pachyderma* is variable about a mean of  $\sim 1.4$  permil and above that level the mean decreases to  $\sim 1.2$  permil. Below  $\sim 15\ \text{cm}$  there is systematic-looking variability in  $\delta^{18}\text{O}$  of *C. lobatulus* individuals of about 0.3 permil. Above that,  $\delta^{18}\text{O}$  decreases, with an abrupt jump in the upper  $\sim 8\ \text{cm}$ .

### 3.5 Alkenone results

Alkenone concentrations increase from about 2000 ng/g at the core bottom to about 3500 ng/g by 10 cm (Fig. 3c). Above 10 cm, they decrease suddenly to 1100 ng/g, and in the upper 2 cm they rise to  $\sim 2500\ \text{ng/g}$ . Alkenone SSTs display an opposite pattern, with a gradual decrease from  $\sim 9.2\ ^\circ\text{C}$  to  $8.4\ ^\circ\text{C}$  by 12 cm. Above 10 cm, SSTs rise dramatically to  $10\ ^\circ\text{C}$ , and then drop again to  $<9\ ^\circ\text{C}$  in the upper 2 cm.

### 3.6 Mg/Ca results

Below 17 cm, Mg/Ca varies within about 10% of  $1.5\ \text{mmol mol}^{-1}$  (Fig. 3e). There is a small increase of  $0.2\ \text{mmol mol}^{-1}$  (equivalent to  $1\ ^\circ\text{C}$ ) between 17 and 4 cm followed by a sharp increase at 3–4 cm. From Lear et al. (in press) we estimate that bottom water temperatures varied between 4 and  $6\ ^\circ\text{C}$  throughout most of the core (Fig. 3e). However, close to the core top, the near doubling of Mg/Ca suggests that bottom water temperature increased to about  $11 \pm 1\ ^\circ\text{C}$  (1 standard error).

## 4 Discussion

With an average linear sedimentation rate of  $30\ \text{cm/kyr}$ , our Emerald Basin core is more than adequate to resolve centennial and even multidecadal scale climate changes. This high accumulation rate must be sustained by the high surface water productivity and ready supply of terrigenous sediments on the various banks surrounding the basin. For example, Kontopoulos and Piper (1982) correlated sand layers among several cores from above 200 m along the southern margin of Emerald Basin and identified them as storm deposits. Near the core top where we have the largest climatic signals, sand grains decrease in abundance (Fig. 3a), and X-radiography of a 350 cm gravity core from the multicore site failed to find any sand layers. As a tracer for fine-grained sedimentation,  $^{210}\text{Pb}$  may indicate an episode of accelerated accumulation, but this is not consistent with transport or reworking of older alkenones. Likewise, low foraminiferal abundance near the core top cannot account for minimum percent abundance of *N. pachyderma* (s.), and minimum  $\delta^{18}\text{O}$ .

Although this is a dynamic sedimentary environment, there is no evidence that sedimentary processes have introduced artifacts into our data set.

All five proxies for seawater temperature reveal a sudden warming within about the past 100 years (Fig. 4), using the calendar age model based on  $^{14}\text{C}$  (Fig. 2). Because the one sigma error is as large as the youngest calibrated date (Table 1), this warming could have begun anytime in the past few hundred years. However, as discussed later, we assume this warming occurred around 150 yrs BP because of the likelihood that it was coincident with the warming known to have occurred in the Canadian archipelago at that time (Koerner and Fisher 1990). In the following sections we will use the tracer data to (1) reconstruct temperature and salinity trends for the past 1600 years in Emerald Basin, (2) evaluate these trends in terms of the instrumental record from this location, and (3) discuss the temperature and salinity trends in terms of changing ocean and climate patterns in the Arctic source for Emerald Basin waters.

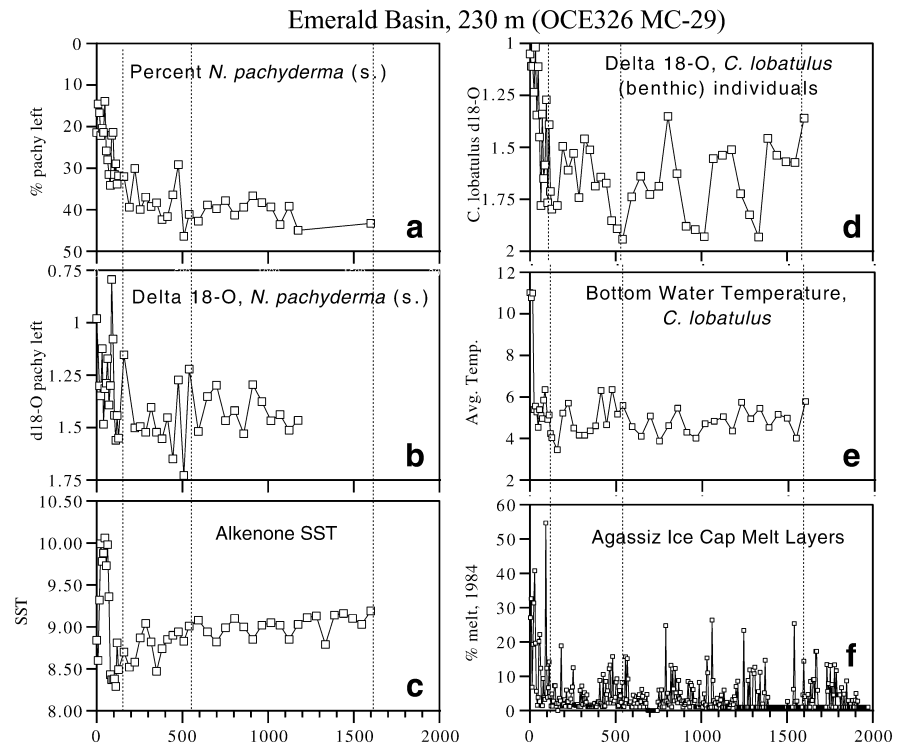
#### 4.1 Temperature and salinity estimation

Among our five proxy indicators for the physical and chemical properties of sea water, we have enough information, in principle, to calculate temperature (T) and salinity (S) for both bottom waters and for surface waters. In practice, this is much more difficult for surface waters than for bottom waters for several reasons. Whereas a large and growing body of evidence indicates that sedimentary alkenone unsaturation ratios (i.e.,  $U_{37}^k$ ) reflect

mean annual SST at 0 m (Müller et al. 1998; Herbert 2001), they may more closely approximate surface water temperature at the time of the prymnesiophyte algae bloom in some locations (see Sikes et al. 1997). The alkenone-derived SSTs may therefore not reflect the same hydrographic conditions sampled by planktonic foraminifera. In addition to possible seasonal differences in population growth, depth habitats of prymnesiophytes and *N. pachyderma* may differ. For instance, the latter is thought to produce the bulk of its calcite at water depths around 50 m (Kohfeld et al. 1996).

Although all our data indicate warming within the past one or two centuries, the individual proxy records differ in detail. For example, decreasing % *N. pachyderma* (Fig. 4a) and its  $\delta^{18}\text{O}$  (Fig. 4b) might reflect 1–2 °C warming in the past 200 years. In contrast, alkenones register abrupt warming of ~1.5 °C only about 100 years ago, followed by an equally abrupt cooling of similar magnitude in recent decades (Fig. 4c). Because the alkenone SST estimate at the core top, ~8.8 °C (Fig. 4e), is in agreement with measured annual average SST during the last half century, we consider  $U_{37}^k$  to accurately reflect SST at this site. Cooling of 1.5 °C in the upper 4 cm of the alkenone record to values typical of the last 1600 years (Figs. 3c and 4c) may be consistent with the surface temperature history of nearby La Have Basin derived from dinoflagellate cysts, but that record may lack the past 100 years (Levac 2001). The decrease of *N. pachyderma*  $\delta^{18}\text{O}$  through the core-top interval (Fig. 4b) may be reconciled with the alkenone-SST decrease if SSS lowered, an inference also supported by dinocyst reconstructions in the La Have Basin (Levac 2001).

**Fig. 4** Comparison of temperature proxy data from Emerald Basin (a–e, as in Fig. 3) and melt layer distribution in Agassiz Ice Cap (f, after Koerner and Fisher 1990). Radiocarbon age control is indicated by dotted vertical lines



Unlike the near-surface ocean proxy data, the benthic data are more amenable to extracting salinity estimates because both Mg/Ca-derived BWT and  $\delta^{18}\text{O}$  were measured on the same species and because there is little seasonality at 250 m in Emerald Basin (Petrie and Drinkwater 1993). The first step in deconvolving salinity from  $\delta^{18}\text{O}$  is to estimate  $\delta_{\text{water}}$  from foraminifera  $\delta^{18}\text{O}$ . Here we assumed that *C. lobatulus* deposits its calcite in equilibrium with  $\delta^{18}\text{O}$  of sea water, an assumption that is supported for other species of *Cibicidoides* by the results of Bemis et al. (1998). We solved the Bemis et al. (1998) equation 1 for the  $\delta^{18}\text{O}$  of seawater, including +0.27‰ to account for the difference between PDB (Pee Dee Belemnite) and SMOW (Standard Mean Ocean Water):

$$\delta_{\text{water}} = ((T - 16.5 + 4.8 \delta_{\text{carb}})/4.8) + 0.27 \text{ ‰}$$

Then, we derived salinity from the equation  $\delta_{\text{water}} = 0.61(\text{Salinity}) - 21$ , the mixing line between Labrador Sea Water and Arctic river water (Khatriwala and Fairbanks 1999). Results of this exercise suggest that bottom water salinities were in the 33–35 psu range for most of the past 1600 years, with two extremes in the last 100 years using our model time scale (Fig. 5a). Sometime in the last 100–200 years bottom water salinities reached below 33 psu, and shortly thereafter they rose to a (core top) maximum of about 35 psu. Evidently, within the uncertainty of the paleotemperature calibrations, core top estimates of bottom water temperature and salinity are consistent with the modern measurements from that site (compare Fig. 5a and b). The recent increase in salinity is probably a robust result because benthic  $\delta^{18}\text{O}$  near the core top is consistently low (Fig. 3d), and the bottom water temperature data are consistently warm (Fig. 3e). However, the preceding salinity minimum might be an artifact of the more scattered  $\delta^{18}\text{O}$  data that decrease before the Mg/Ca data increase.

Although the sudden jump in nineteenth century SST and BWT, and bottom water salinity, are the most striking feature of our results, we should note that there are smaller changes of possible significance during earlier centuries. For example, alkenone SSTs indicate small cold events every few hundred years (Fig. 4c), benthic  $\delta^{18}\text{O}$  oscillated between 500 and 1500 years ago (Fig. 4d), and bottom water temperatures varied concomitantly by 1–2 °C (Fig. 4e). Variability in the benthic data combine to indicate maxima in bottom water temperature and salinity about 200, 500, 1000, and 1300 years ago (Fig. 5a). Our surface and deep water proxy results all suggest that sampling strategies should be chosen to maximize the likelihood of resolving multi-decadal to centennial climate changes from nearshore sediments.

#### 4.2 Emerald Basin and the Labrador Current

Emerald Basin waters are influenced by either the near-shore cool and fresh Labrador slope waters, or the

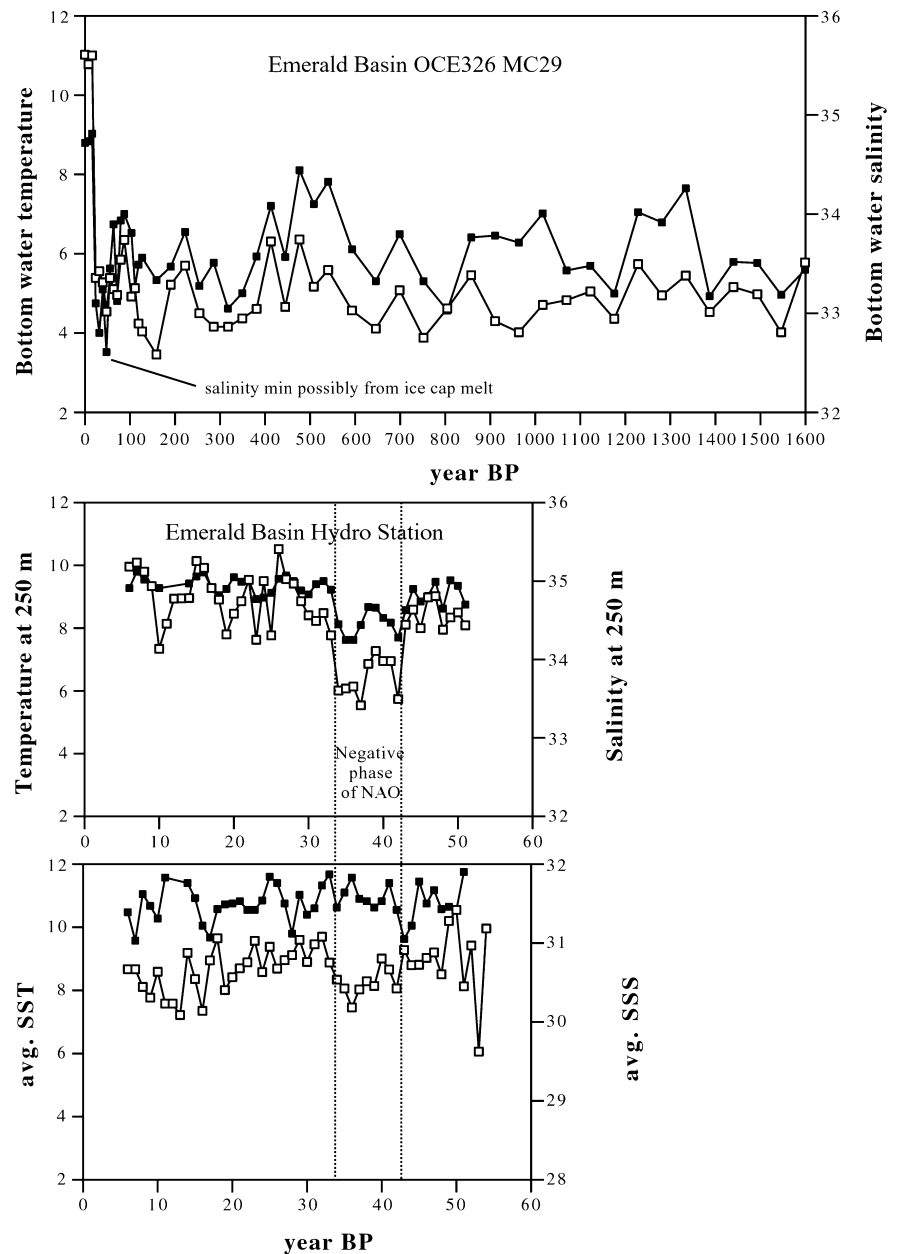
offshore warm slope waters (Gatien 1976). The extent of Labrador slope waters appears to be driven by transport of the Labrador Current. Over the course of more than fifty years of monthly observations, interdecadal changes in Emerald Basin waters are well documented (Petrie and Drinkwater 1993; Fig. 5b and c). The largest hydrographic change in this long series occurred during the late 1950s and 1960s, when the North Atlantic Oscillation was in its strongest negative phase (Fig. 5b and c). At that time annual average BWT was nearly 5 °C lower than today, and salinities were about 0.7 psu lower. There is very little seasonality in the deep Emerald Basin, whereas near surface waters are coastal in origin and are more affected by weather than the deep waters (Petrie and Drinkwater 1993). On an annual average, SST was little affected by the 1960s NAO minimum, whereas 15 years ago SST was actually lower than BWT. Under these circumstances, we should not necessarily expect surface and deep T and S trends to be identical.

Petrie and Drinkwater (1993) discuss two alternative explanations for the low frequency climate changes deep in Emerald Basin. Although it is clear that there was a greater influence of Labrador slope waters in Emerald Basin during the 1960s, this could have resulted from either lower temperature and salinity in the Labrador Current itself, or greater transport of the Labrador Current. They concluded that increased transport of the Labrador Current was responsible because even though the Labrador Current was slightly warmer and saltier during the 1950s and 1960s than it is today, it was continually colder and fresher than the slope waters off Nova Scotia. Accordingly, it is reasonable to compare our proxy data for temperature and salinity increase during the nineteenth century with the changes measured by instruments during the 1960s.

The striking rise in BWT that began during the nineteenth century is comparable in magnitude to what was observed at the end of the 1960s (Fig. 5). Our reconstruction shows a temperature increase from  $\sim 5$  to  $\sim 11 \pm 1$  °C, consistent (within 1 standard error of the estimate) with the instrumental observations of an annual average increase from  $< 6$  to  $> 10$  °C. The paleosalinity data are generally fresher than the modern data for most of the past 1600 years, with a recent increase to modern salinities ( $\sim 35$  psu). Building on the interpretations of Petrie and Drinkwater (1993), we suggest that from 1600 years BP until the middle 1800s the Labrador Current was fresher and colder than today, and in a high transport mode.

Our evidence for rapid warming of the surface ocean (*N. pachyderma* (s.) abundance data, stable isotope data, and alkenone data) during the nineteenth century is also consistent with historical trends. Although SST decreased by  $\sim 1.5$  °C from 50 to 35 years ago, the instrumental data also show that there was no permanent shift in SST resulting from the negative NAO (Fig. 5c). More recently, surface waters have been just as cold, and it is possible that the alkenone evidence for cooling near the core top (Fig. 4c) may have captured one of those events. We

**Fig. 5a–c** Comparison of proxy data for bottom water temperature and salinity in Emerald Basin with instrumental data (provided by K. Drinkwater, Bedford Institute of Oceanography). In **a**, note the general covariance between BWT and BWS, except for samples dated to about 50 years ago. As discussed in the text, this part of the core probably records changes that occurred  $\sim 100$  years ago. At that time, the uncoupling of BWT and BWS could have been a dynamic response to local melting and freshening in the Canadian archipelago (Koerner 1977; Koerner and Fisher 1990). From **b**, instrumental data at the bottom of the basin, it is seen that BWT depression during the minimum phase of the NAO was similar to the all of the paleo record but the past  $\sim 100$  years, and that **c** changes in SST of 1–2 °C are common and not necessarily tied to BWT



conclude that persistent intrusion of Labrador Current waters into Emerald Basin for most of the past 1600 years and local surface ocean and atmosphere cooling probably had the same cause. These conditions would seem to be consistent with a very long Little Ice Age, perhaps because there is no evidence whatsoever for a Medieval Warm Period in the waters off Nova Scotia.

#### 4.3 Arctic influence on the Labrador Current

Waters of the equator-flowing Labrador Current have two main sources, each of Arctic origin (Lazier and Wright 1993; Loder et al. 1998; Fig. 1). One flow enters the Nordic Sea from Fram Strait and follows the coast from east to west Greenland. In the northern Labrador

Sea, a branch of the West Greenland Current turns westward and is joined by a second arctic flow through the Canadian archipelago and out Davis Strait. Because there are two distal sources for the waters that make up the Labrador Current, it is possible that changing conditions in one region or the other could account for the step-like increase in  $T$  and  $S$  in Emerald Basin. Waters of the West Greenland Current are warmer and saltier than the waters exiting Davis Strait because of mixing with North Atlantic waters in the Irminger Sea. However, these differences are small (in the instrumental record) and probably cannot account for the large changes we infer for Emerald Basin in the nineteenth century.

Ice cores provide direct evidence that there was atmospheric warming in northern Baffin Bay region that should have affected Arctic waters running south

through Davis Strait (the Baffin Island Current). It is this warming, which is more accurately dated in ice cores than in Emerald Basin, that we believe is probably synchronous with and the cause of the warming we observe in the Emerald Basin. Koerner (1977) first showed that the Devon Ice Cap experienced post-Little Ice Age melting beginning about 1860, with accelerated melting in the 1920s. This observation was later confirmed by Koerner and Fisher (1990) at Agassiz Ice Cap, where they showed very few ice-melt layers for several thousand years prior to the sudden warming that occurred there beginning  $\sim$ 1890 (Fig. 4f). The accelerated melting of the regional ice caps, as well as the melting of local snow carried on sea ice, might account for our observation of minimum salinity in Emerald Basin just before the increase in both  $T$  and  $S$  (Fig. 5a). Furthermore, because the Labrador Current is buoyancy driven (Lazier and Wright 1993), a sudden decrease in Baffin Island Current salinity would increase the steric height of the waters over the continental shelf with respect to the open Labrador Sea. This in turn might have temporarily increased the transport of the Labrador Current, and incursion of those cold deep waters into Emerald Basin, and could account for some of the lag in bottom water warming (Fig. 4e) with respect to surface warming in the proxy data (Fig. 4a–c).

From various lines of proxy evidence around the Arctic, it is now known that the abrupt warming in the nineteenth century marked the end of the Little Ice Age (Overpeck et al. 1997). However, the proxy data assembled by Overpeck et al. (1997) include only one marine record, that of Jennings and Weiner (1996) from a fjord in East Greenland. Those authors used the abundance of a benthic foraminiferal species to infer the presence of warmer and saltier Atlantic water during the Medieval Warm Period. Medieval warming is well known in both East and West Greenland, because that is when Norse colonies were established (Dansgaard et al. 1975). However, our Emerald Basin results show no evidence of medieval warming much farther to the southwest. This supports the notion that for most of the past 1600 years the Labrador Current was dominated by the Canadian archipelago source.

The preceding paragraphs attempt to make the case that the long cold and fresh interval in Emerald Basin can be explained by persistent influence of Baffin Bay waters on the Labrador Current. This circulation regime is sketched in Fig. 6a and c. But what caused the abrupt warming in Emerald Basin? As suggested, one answer is that during the past 150 years or so the average transport of the Labrador Current decreased, and the cold slope waters were unable to displace the warm slope waters (except during relatively brief intervals of negative NAO).

However, there is also direct evidence for a change in the source waters of the Labrador Current. The distribution of driftwood around the Arctic has been used to infer changes in the position of the transpolar drift during the Holocene (Dyke et al. 1997; Tremblay et al.

1997). Changes in the transpolar drift, in turn, probably reflect long-term shifts in the dominant mode of wind-forced circulation that are known to occur in the Arctic on interannual time scales today (Proshutinsky and Johnson 1997). For most of the past 4000 years, essentially the Neoglacial period, Dyke et al. (1997) found that there was a strong dominance of North American wood in the Canadian Arctic archipelago, and a dearth of wood reaching Baffin Bay. This pattern is evidence for a westward position of the transpolar drift (Fig. 6a), such that little driftwood exited Fram Strait and found its way to Baffin Bay via the West Greenland Current. Beginning about 250 years ago, there is increased evidence of wood arrival in Baffin Bay. Dyke et al. (1997) interpret this condition to reflect *the eastward movement to an intermediate position of the transpolar drift*. Because they binned their wood samples into 250 year intervals, it is not clear exactly when this shift occurred, but it does suggest that sometime recently there was probably a greater influence of the West Greenland Current in the mix of waters that make up the Labrador Current. This could have contributed to the recent warming that we have found in the Emerald Basin if relatively warm Irminger Sea waters contributed to the West Greenland Current.

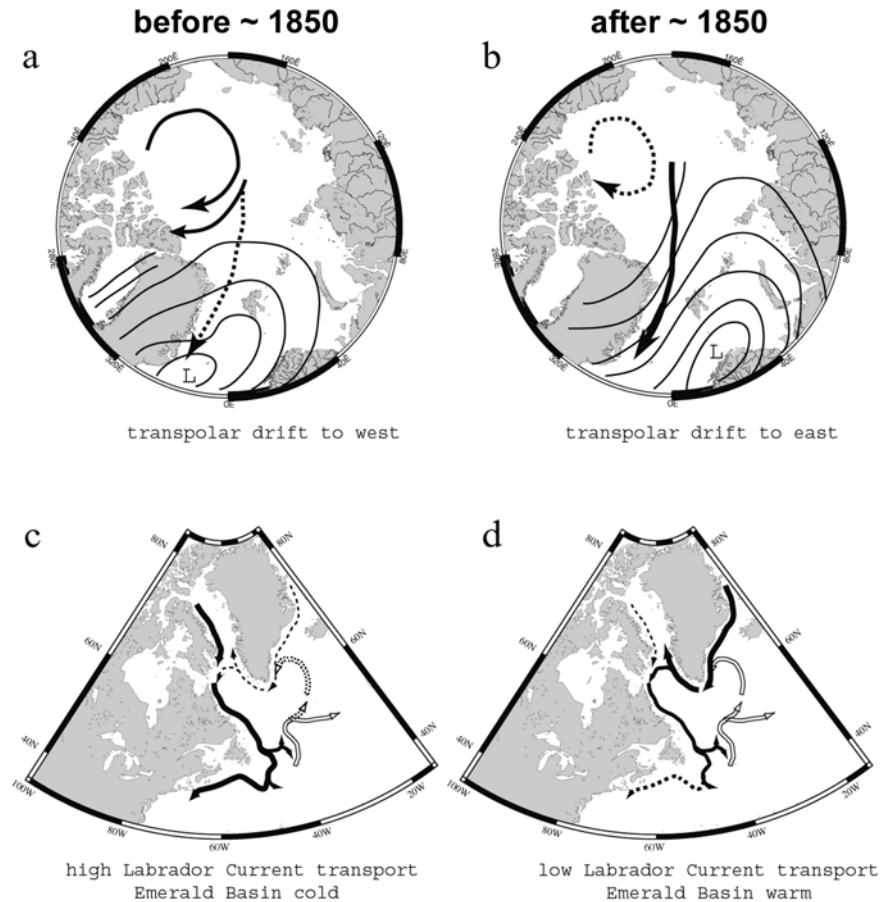
It is worth noting here that Tremblay et al. (1997) have modeled the Arctic Ocean response to different atmospheric forcings, to account for shifts in the position of the transpolar drift. They find that the *eastern* end member of the transpolar drift, that would enhance the Fram Strait source of the Labrador Current (Fig. 6b), is consistent with the negative phase of the NAO. This relationship is opposite to that proposed based on the instrumental observations in Emerald Basin, where maximum Labrador Current flow (Fig. 6c) occurred during the NAO negative phase (Petrie and Drinkwater 1993). *In other words, the atmospheric and surface ocean circulation patterns sketched in Fig. 6 cannot easily be reconciled with NAO forcing*. Although there could be many explanations for this contradiction, for now it is important to bear in mind that it may not be entirely appropriate to use the modern NAO, an interdecadal phenomenon, as a model for century- and millennial-scale processes. This was underscored recently by deMenocal et al. (2000) who noted that increased upwelling off West Africa during the Little Ice Age was inconsistent with the idea that the LIA could have been an extended minimum phase of the NAO (Keigwin 1996).

## 5 Conclusions

Although basins on continental shelves are subject to severe bioturbation from the high surface ocean fertility, to sediment resuspension from storms, and to sediment disturbance from fishing and gas seepage, our various paleo data sets indicate that Emerald Basin sediments contain a very high resolution record of recent climate



**Fig. 6a–d** Sketches showing patterns of atmospheric forcing and surface ocean circulation that might account for sudden warming in the Emerald Basin in the nineteenth century, after 1500 years of cold and fresh conditions. The atmospheric pressure patterns and response of the transpolar drift (*upper illustrations*) are based on the ideas of Tremblay et al. (1997) and Proshutinsky and Johnson (1997). Stronger surface currents are suggested by *bold lines*, and weaker currents by *dashed or dotted lines*



and ocean change. Such locations should be sampled at centimeter spacing in order to extract the most information. The principal feature we have identified using five proxies for ocean temperatures is an abrupt warming of SST by 1.5 °C and of bottom waters by ~5 °C in the upper 10 cm of our multicore. Our radiocarbon age model indicates these changes occurred within the past century, but radiocarbon dating is notoriously inaccurate in recent centuries. Instead, by correlation with the records of ice core melt layers in the Canadian archipelago (Koerner 1977; Koerner and Fisher 1990) and other paleo data (Overpeck et al. 1997), we suggest that this warming occurred in the middle of the nineteenth century. For about 15 centuries before this warming, bottom water temperatures were about 5 °C colder and bottom water salinities were lower by about 1 psu than today. SSTs declined in this interval from ~9 °C to <8.5 °C. There is no evidence for a Medieval Warm Period in Emerald Basin waters, and the cold and fresh conditions in this 1500 year interval were similar to those recorded in Emerald Basin during the 1960s negative phase of the North Atlantic Oscillation (Petrie and Drinkwater 1993).

Despite the consistent evidence for warming sometime in the nineteenth century, our various proxy results differ in important details. For example, surface water warming occurred before bottom water warming, and

the alkenone SST record indicates cooling at the top of the core to the pre-nineteenth century situation. We suspect that these differences reflect the much greater seasonal and interannual variability in surface waters than in deep waters. Recent cooling of Emerald Basin SSTs must be real because the alkenone SST data converge with existing instrumental data.

Following the Petrie and Drinkwater (1993) analysis of the long series of Emerald Basin hydrographic data, we attribute much of the change observed in the past 150 years or so to departure of Labrador Current waters from the Scotian shelf. Thus, the increase in bottom water temperature and salinity in Emerald Basin is probably related to decreased flux and changing hydrography of the Labrador Current. Changes in hydrography and transport could have resulted from two processes: (1) recent warming and icecap melting in the northern Baffin Bay region, and (2) switches between the Canadian archipelago and Fram Strait headwaters of the Labrador Current.

**Acknowledgements** We acknowledge NSF grants OCE9709686 to LDK for OCE voyage 326 and associated laboratory work, and OCE9819675 to YR. We acknowledge the MIT Wade Fund and a Doherty Professorship for providing funding for this work to JPS. We also thank Eben Franks for his coring skills at sea, and for his operation of the mass spectrometer, and Ellen Roosen for her micropaleontology skills; Ying Chang for assistance with alkenone

analyses; the AMS facility at WHOI, Ken Buesseler for  $^{210}\text{Pb}$  dating; and Kate Moran, David Piper, and Iris Hardy for discussions about core locations on the Canadian margin and for providing samples. In particular, Kate Moran recommended the location of MC-29. We thank David Piper and Lawrence Mysak for reviews of the manuscript, and Mysak's suggestion to add Fig. 6.

## References

- Bemis BE, Spero HJ, Bijma J, Lea DW (1998) Reevaluation of the oxygen isotopic composition of planktonic foraminifera: experimental results and revised paleotemperature equations. *Paleoceanography* 13: 150–160
- Boyle EA, Keigwin LD (1985/86) Comparison of Atlantic and Pacific paleochemical records for the last 215,000 years: changes in deep ocean circulation and chemical inventories. *Earth Planet Sci Lett* 76: 135–150
- Dansgaard W, Johnsen SJ, Reeh N, Gundestrup N, Calusen HB, Hammer CU (1975) Climatic changes, Norsemen and modern man. *Nature* 255: 24–28
- deMenocal P, Ortiz J, Guilderson T, Sarnthein M (2000) Coherent high- and low-latitude climate variability during the Holocene warm period. *Science* 288: 2198–2202
- Dyke AS, England J, Reimnitz E, Jette H (1997) Changes in driftwood delivery to the Canadian Arctic Archipelago: the hypothesis of postglacial oscillations of the Transpolar Drift. *Arctic* 50: 1–16
- Gatien MG (1976) A study in the slope water region south of Halifax. *J Fish Res Board Can* 33: 2213–2217
- Herbert TD (2001) Review of alkenone calibrations (culture, water column, and sediments). *Geochem Geophys Geosyst* 2: 2000GC000055
- Jennings AE, Weiner NJ (1996) Environmental change in eastern Greenland during the last 1300 years: evidence from foraminifera and lithofacies in Nansen Fjord, 68°N. *The Holocene* 6: 179–191
- Keigwin LD (1996) The little ice age and medieval warm period in the Sargasso Sea. *Science* 274: 1504–1508
- Khatiwalala SP, Fairbanks RG, Houghton RW (1999) Freshwater sources to the coastal ocean off northeastern North America: evidence from  $\text{H}_2^{18}\text{O}/\text{H}_2^{16}\text{O}$ . *J Geophys Res* 104: 18,241–18,255
- King LH, Fader GBJ (1986) Wisconsinan glaciation of the Atlantic continental shelf of southeast Canada. *Geological Survey of Canada*, pp 1–72
- Koerner RM (1977) Devon Island ice cap: core stratigraphy and paleoclimate. *Science* 196: 15–18
- Koerner RM, Fisher DA (1990) A record of Holocene summer climate from a Canadian high-Arctic ice core. *Nature* 343: 630–631
- Kohfeld KE, Fairbanks RG, Smith SL, Walsh ID (1996) *Neoglobobulimina pachyderma* (sinistral coiling) as paleoceanographic tracers in polar oceans: Evidence from Northeast Water Polynya plankton tows, sediment traps, and surface sediments. *Paleoceanography* 11: 679–699
- Kontopoulos N, Piper DJW (1982) Storm graded sand at 200 m water depth, Scotian Shelf, eastern Canada. *Geo-Marine Lett* 2: 77–81
- Lazier JRN, Wright DG (1993) Annual velocity variations in the Labrador Current. *J Phys Oceanogr* 23: 659–678
- Lear CH, Rosenthal Y, Slowey N (2002) Benthic foraminiferal Mg/Ca-paleothermometry: a revised core-top calibration. *Geochim Cosmochim Acta* (in press)
- Levac E (2001) High resolution Holocene palynological record from the Scotian Shelf. *Mar Micropaleo* 43: 179–197
- Loder JW, Petrie B, Gawarkiewicz G (1998) The coastal ocean off northeastern North America: a large-scale view. In: Robinson AR, Brink KH (eds) *The sea*. John Wiley, 11, pp 105–133
- Müller PJ, Kirst G, Ruhland G, von Storch I, Rosell-Mele A (1998) Calibration of the alkenone paleotemperature index  $\text{U}^{\text{k}}_{37}$  based on core-tops from the eastern South Atlantic and the global ocean (60°N–60°S). *Geochim Cosmochim Acta* 62: 1757–1772
- Overpeck J, Hughen K, Hardy D, Bradley R, Case R, Douglas M, Finney B, Gajewski K, Jacoby G, Jennings A, Lamoureux S, Lasca A, MacDonald G, Moore J, Retelle M, Smith S, Wolfe A, Zielinski G (1997) Arctic environmental changes of the last four centuries. *Science* 278: 1251–1256
- Petrie B, Drinkwater K (1993) Temperature and salinity variability on the Scotian Shelf and in the Gulf of Maine 1945–1990. *J Geophys Res* 98: 20,079–20,089
- Piper DJW, Fehr SD (1991) Radiocarbon chronology of late Quaternary sections on the inner and middle Scotian Shelf, south of Nova Scotia. *Current Research, Part E; Geological Survey of Canada*, pp 321–325
- Prahl FL, Muehlhausen L, Zahnle D (1988) Further evaluation of long-chain alkenones as indicators of paleoceanographic conditions. *Geochim Cosmochim Acta* 52: 2303–2310
- Proshutinsky AV, Johnson MA (1997) Two circulation regimes of the wind-driven Arctic Ocean. *J Geophys Res* 102: 12,493–12,514
- Rosenthal Y, Field P, Sherrell R (1999) Precise determination of element/calcium ratios in calcareous samples using sector field inductively coupled plasma mass spectrometry. *Analyt Chem* 71: 3248–3253
- Sachs JP, Lehman SJ (1999) Subtropical North Atlantic temperatures 60,000 to 30,000 years ago. *Science* 286: 756–759
- Scott DB, Mudie PJ, Vilks G, Younger DC (1984) Latest Pleistocene–Holocene paleoceanographic trends on the continental margin of eastern Canada: foraminiferal dinoflagellate and pollen evidence. *Mar Micropaleo* 9: 181–218
- Sikes EL, Volkman JK, Robertson LG, Pichon J-J (1997) Alkenones and alkenes in surface waters and sediments of the Southern Ocean: implications for paleotemperature estimation in polar regions. *Geochim Cosmochim Acta* 61: 1495–1505
- Tremblay L-B, Mysak LA, Dyke AS (1997) Evidence from driftwood records for century-to-millennial scale variations of the high latitude atmospheric circulation during the Holocene. *Geophys Res Lett* 24: 2027–2030
- Vilks G, Rashid MA (1976) Post-glacial paleo-oceanography of Emerald Basin, Scotian Shelf. *Can J Earth Sci* 13: 1256–1267